Probabilistic Lifetime Prediction of Electronic Packages Using Advanced Uncertainty Propagation Analysis and Model Calibration

Hyunseok Oh, Hsiu-Ping Wei, Bongtae Han, and Byeng D. Youn

***Abstract*— We propose a novel methodology for calibrating the physics-based lifetime models of the electronic packages using the eigenvector dimension-reduction (EDR) method and a censored data analysis. The methodology enables to overcome two challenges that are encountered in typical electronic packaging applications: 1) the minimum computational cost without sacrificing the prediction accuracy and 2) the proper handling of the censored data. The EDR method is first employed for uncertainty propagation for the computational efficiency when multiple unknown variables are to be used in nonlinear damage models. Next, the likelihood function is modified to handle the failure data as well as the censored data in the likelihood analysis, and thus establishes the correlation between the model response and the experimental result. Finally, through an unconstrained optimization process, a calibrated parameter set of statistical distributions for unknown input variables is obtained while maximizing the modified likelihood. The proposed statistical calibration approach is implemented for solder joint fatigue reliability. The results confirm the claimed computational effectiveness for an accurate physics-based lifetime model.**

***Index Terms*— Censored data, eigenvector dimension reduction (EDR), modified maximum likelihood, probabilistic physics-based lifetime model, statistical calibration, uncertainty propagation.**

I. Introduction

THE ACTUAL lifetime of an electronic product varies due to inherent variability in materials, geometries, and operation conditions [1]. The physics-based lifetime modeling can assess the statistical distribution of the product lifetime. The statistical distribution, if predicted accurately, can be effectively used to identify the potential safety risks and to calculate the warranty and the maintenance costs [2]. Numerous studies have demonstrated the effectiveness of the probabilistic approach in the physics-based lifetime modeling [3]–[6].

The statistical distribution of the product lifetime can be obtained by the uncertainty propagation analysis. Extensive efforts have been made to achieve high accuracy without compromising the computational cost. The methods for the uncertainty propagation analysis can be categorized into: 1) random sampling; 2) expansion; 3) response surface; and 4) approximate integration methods. Table I summarizes the pros and cons of the existing methods.

Among the methods, the conventional Monte Carlo simulation technique (random sampling) usually offers the most accurate results [7]. However, it is not suitable to some engineering problems for which the computational cost is extremely high. The Monte Carlo simulation technique combined with Latin hypercube sampling can be used to relieve the computational burden [8], [9]. More rigorously, the adoption of the response surface approximation technique with Monte Carlo sampling is widely accepted to reduce the computational burden significantly [10], [11]. Yet, the accuracy of their outputs depends on how accurately the response surface is constructed. In addition, the Monte Carlo simulation and the response surface approximation techniques suffer from the curse of dimensionality. The computational cost increases exponentially as the number of variables increases.

The expansion method is effective when the uncertainty in input variables is relatively small. To account for a large deviation in input variables, higher order terms should be incorporated in the expansion, which increases the computational cost exponentially with the increased number of input variables. Its application is limited to the cases where the input variables follow Gaussian distributions.

The approximate integration method is relatively new but it has a distinct advantage over other methods [12], [13]. The computational cost increases only additively with the increased number of variables, since the statistical moments are calculated by the additive decomposition of a multiple-

Manuscript received May 11, 2015; revised September 23, 2015; accepted December 15, 2015. Date of publication January 13, 2016; date of current version February 5, 2016. This work was supported by the Korea Institute of Energy Technology Evaluation and Planning under Grant 20118520020010 and by the Technology Innovation Program (10048305, Launching Plug-in Digital Analysis Framework for Modular system Design) of the Ministry of Trade, Industry & Energy (MI, Korea). Recommended for publication by Associate Editor C. J. Bailey upon evaluation of reviewers' comments. *(Corresponding authors: Hyunseok Oh and Bongtae Han.)*

H. Oh was with the Department of Mechanical Engineering, University of Maryland, College Park, MD 20742 USA. He is now with the Department of Mechanical Engineering, Seoul National University, Seoul 151-742, Korea (e-mail: hyunseok52@gmail.com).

H.-P. Wei and B. Han are with the Department of Mechanical Engineering, University of Maryland, College Park, MD 20742 USA (e-mail: hsiupingwei@gmail.com; bthan@umd.edu).

B. D. Youn is with the Department of Mechanical Engineering, Seoul National University, Seoul 151-742, Korea (e-mail: bdyoun@snu.ac.kr).

Color versions of one or more of the figures in this paper are available online at http://ieeexplore.ieee.org.

Digital Object Identifier 10.1109/TCPMT.2015.2510398

TABLE I
PROS AND CONS OF UNCERTAINTY PROPAGATION METHODS

	Examples	Pros	Cons
Random sampling	· Monte Carlo simulation · Monte Carlo simulation with Latin hypercube sampling	· Most accurate	· Most computationally expensive
Response surface	· Response surface method with Monte Carlo simulation	· The number of runs can be reduced by DOE sampling.	· The accuracy depends on the accuracy of a response surface. · Curse of dimensionality: computational costs increase exponentially with the increase of the number of variables.
Expansion	· Second order Taylor approximation	· Simple to implement	· The result can be inaccurate when input uncertainty is high and a density function is non-Gaussian.
Approximate integration	· Univariate dimension reduction · Eigenvector dimension reduction	· Affordable computational costs	· Additive decomposition adds potential uncertainty. · The numerical implementation of one-dimensional integration can affect the accuracy.

dimensional integration; the calculation error of the statistical moments by the additive decomposition has been proved to be smaller than that of the second-order Tayler series expansion [12]. Among various approximate integration methods, the eigenvector dimension-reduction (EDR) method is known to be effective for the uncertainty propagation analysis for nonlinear damage models, since it requires a fewer number of sampling points without compromising the accuracy [13].

Uncertainties are inherent during the statistical calibration of physics-based lifetime modeling. They can be categorized into physical uncertainty and model uncertainty. Physical uncertainty comes from inherent randomness in material properties, product geometries, and loading conditions, whereas model uncertainty is attributed to the lack of an accurate model that emulates actual failure mechanisms. In general, experimental quantification of physical uncertainty is an expensive and time-consuming task [14], [15], while expert knowledge and/or reference information is sometimes used to speculate physical uncertainty. However, the use of inaccurate information in physics-based lifetime modeling can compromise the predictive capability of a model, albeit not intentionally. To this end, it is desirable to develop a practical strategy that results in a high-fidelity physics-based lifetime model.

The concept of statistical calibration was developed to improve the accuracy of computational models in the engineering design community. Model calibration is defined as an activity that adjusts a set of unknown parameters in a computational model to maximize the agreement between the outputs from simulation and experiments [16], [17]. The approach is considered as a practical and feasible way for assessing the uncertainty in computational modeling. The statistical model calibration requires multiple sample data, since a valid conclusion from a statistical analysis can be drawn only with a sufficient number of samples; the optimal number of samples for statistical analysis of life testing data varies depending on applications. In addition, the competitive market environment often dictates the testing time, which results in surviving samples (i.e., censored or suspension data) at the termination of testing. The need to consider censored data as well as failure data has been underscored by the ever-decreasing product development cycle time. To the best of our knowledge, the previous model calibration studies did not address this issue.

To overcome the above challenges, namely, the minimum computational cost without sacrificing the prediction accuracy and the proper handling of the censored data, this paper proposes a novel methodology for calibrating physics-based lifetime models using the EDR method and a censored data analysis. Section II presents the key theories that are used in the proposed methodology. In Section III, the methodology is described for statistical calibration in probabilistic physics-based lifetime modeling. Section IV reports the results from a case study to demonstrate the effectiveness of the proposed methodology. Section V concludes this paper with the future work.

II. THEORETICAL BACKGROUND

This section reviews two key methods used in the proposed methodology: 1) the EDR method and 2) the likelihood analysis with failure data as well as censored data.

A. Eigenvector Dimension-Reduction Method for Uncertainty Propagation

An uncertainty propagation analysis using the approximate integration method is achieved by: 1) calculating the statistical moments of a system response and 2) constructing the statistical distributions of the system response using the

statistical moments. The mth-order statistical moment of a system response is defined as

$$E\{Y^m(X)\} \equiv \int_{-\infty}^{+\infty} \cdots \int_{-\infty}^{+\infty} \{y(x_1, \ldots, x_N)\}^m \times f_{x_1,\ldots,x_N}(x_1, \ldots, x_N) dx_1, \ldots, dx_N \quad (1)$$

where $E(\cdot)$ is the expectation operator, $Y(X) = y(x_1, \ldots, x_N)$ is the system response function with N random variables, $X = x_1, \ldots, x_N$ (i.e., N dimension), and $f_{x_1,\ldots,x_N}(x_1, \ldots, x_N)$ is the joint probability density function (pdf).

Equation (1) poses a mathematical challenge in executing a multidimensional integration. To address this challenge, Rahman and Xu [12] proposed a novel concept of additive decomposition, which is to approximate a multidimensional response function into multiple 1-D functions. When (1) is additively decomposed, one obtains

$$E\{Y^m(X)\} \cong E\left\{\left[\sum_{j=1}^{N} y(\mu_1, \ldots, \mu_{j-1}, x_j, \mu_{j+1}, \ldots, \mu_N) - (N-1)y(\mu_1, \ldots, \mu_N)\right]^m\right\} \quad (2)$$

where μ_j is the mean of x_j. By binomial and recursive formulas, the right-hand side of (2) becomes

$$\sum_{i=0}^{m} \binom{m}{i} S_N^i [-(N-1)y(\mu_1, \ldots, \mu_N)]^{m-i} \quad (3)$$

where

$$S_1^i = E\{[y(x_1, \mu_2, \ldots, \mu_N)]^i\}$$

$$S_j^i = \sum_{k=0}^{i} \binom{i}{k} S_{j-1}^k E\{[y(\mu_1, \ldots, \mu_{j-1}, x_j, \mu_{j+1}, \ldots, \mu_N)]^{i-k}\}$$

and

$$S_N^i = \sum_{k=0}^{i} \binom{i}{k} S_{N-1}^k E\{[y(\mu_1 \ldots, \mu_{N-1}, x_N)]^{i-k}\}.$$

The EDR method employs three steps in calculating the expectation of the 1-D numerical integration [13]: 1) the eigenvector sampling approach to determine the integration points; 2) the stepwise moving least square method to construct an approximated 1-D response curve for the mth-order function of x_j; and 3) the adaptive Simpson rule to form a numerical integration equation of an approximated response curve. It should be noted that Steps 2) and 3) may accumulate a small amount of numerical error but it is expected to be negligible [13]. Once the first four statistical moments of a system response are obtained using (3), the Pearson system constructs the statistical distribution (i.e., pdf) of a random response, y, which is the final outcome of the EDR method for an uncertainty propagation analysis.

The EDR method only requires $(2N + 1)$ or $(4N + 1)$ runs of a computational model. The choice for either $(2N + 1)$ or $(4N + 1)$ depends on the degree of system response nonlinearity. With additive decomposition, the computational cost for the EDR method increases only additively as the number of variables increases, avoiding the curse of dimensionality. This is the major advantage over the response surface, expansion, Monte Carlo simulation techniques, and their combinations.

B. Modified Likelihood for Failure Data and Censored Data

A metric should be defined to quantify the degree of agreement between two pdfs obtained from modeling and experiments. In the literature, three types of metrics are found: 1) mean squared error [18]; 2) Bayesian measure [19], [20]; and 3) likelihood [17], [21]. The mean squared error metric is easy to calculate, whereas variability of individual samples in the experiments is not accounted for. When a small number of samples are available, the Bayesian measure can provide a more accurate estimate than the mean square error metric. However, the accuracy of a Bayesian measure relies on that of the prior information that the user has to determine. The likelihood directly quantifies the correlation between the variability in the experiments and a pdf calculated by a model; yet, its computational cost is lower than the Bayesian measure. For these reasons, the likelihood is widely used as an efficient metric for the statistical model calibration of engineering systems.

Assuming k independent samples used in a life test, a likelihood function is defined as

$$L(p; t_1, \ldots, t_k) = C \prod_{i=1}^{k} L_i(p; t_i) \quad (4)$$

where $L_i(p;t_i)$ is the probability of the ith failure, C is the constant, t_i is the time-to-failure [or cycles-to-failure (CTF)] of the ith failure, and p is the vector of parameters of the pdf.

In a life test, it is not unusual to have censored data whose exact failure time is unknown. Left censoring means that a failure occurs before the first inspection. Interval censoring implies that a failure occurs between inspections. Right censoring indicates that a failure is known to occur after the termination of life testing [22]. A likelihood function with censored data is [22]

$$L(p; t_1, \ldots, t_k) \propto \prod_{i=1}^{k} [F(t_i)]^{l_i} [F(t_i) - F(t_{i-1})]^{d_i} [1 - F(t_i)]^{r_i} \quad (5)$$

where $F(t_i)$ is the cumulative distribution function (cdf) of t_i, and l_i, d_i, and r_i are 1 if the ith sample is either left, interval, or right censored, respectively. Otherwise, l_i, d_i, and r_i are set to be zero. The sum of l_i, d_i, and r_i is the total number of samples (k) in a life test.

III. Methodology for Statistical Calibration of Physics-Based Lifetime Model

The flowchart of the proposed methodology is shown in Fig. 1; the main parts include physics-based lifetime modeling, uncertainty propagation, and likelihood calculation. The physics-based lifetime modeling consists of life modeling and damage modeling. Numerous life models have been

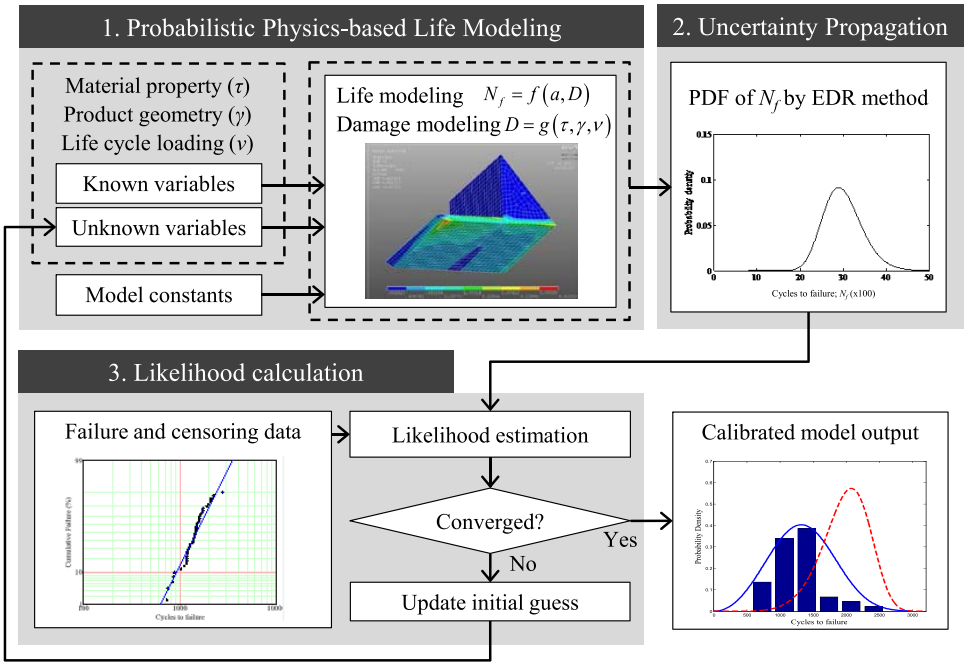

Fig. 1. Flowchart of the proposed methodology.

developed to emulate failure mechanisms. Some of the well-known models for the reliability of semiconductor packages are summarized in Table II.

The functional relationship between life and damage at a potential failure site is determined. The relationship can be expressed as

$$\hat{T}_f = f(a, D) \tag{6}$$

where $\hat{T}_f$ is the lifetime predicted from a life model, a is the vector of model parameters, and D is the damage index. Model parameters are typically estimated by fitting the experimental data into a relevant life model.

Next, damage modeling determines the damage at the potential failure site of an engineering system subjected to environmental and operational loadings. The functional relationship can be expressed as

$$D = g(\tau, \gamma, \nu) \tag{7}$$

where τ is the vector that consists of product geometry variables, γ is the vector that consists of manufacturing process variables, and ν is the vector that consists of environmental and operational loading variables. Damage modeling can be completed by adopting a linear damage accumulation law (e.g., Miner's rule) or using commercial finite-element analysis tools (e.g., ABAQUS and ANSYS). The outcome from life and damage modeling is the predicted lifetime of an engineering system/component.

Uncertainties in material properties, product geometries, and environmental and operational loadings always exist due to inherent randomness. In this paper, uncertain parameters in material properties, product geometries, and loadings are referred to as unknown variables. They should be distinguished from known variables whose variability is known a priori. An initial guess of unknown variables can be made in a parametric form of a pdf. Initial pdfs of unknown variables can be assumed by reviewing the literature or referring to experts' opinions.

When inherent uncertainty in unknown variables is incorporated into the damage model and subsequently into the life model, a pdf of lifetimes is expected to be an output response of a probabilistic physics-based life model. As discussed in Section II-A, uncertainty propagation requires a significant amount of computational resources. The EDR method is employed in this paper for the reasons mentioned earlier.

The correlation between the predicted and experimental results can be maximized with an objective function of the likelihood. In a life testing, interval- and right-censored data are typically observed, whereas left-censored data are not common. Therefore, the objective function for the optimization is defined as

$$L(p; t_1, \ldots, t_k) \propto \prod_{i=1}^{k} [F(t_i) - F(t_{i-1})]^{d_i} [1 - F(t_i)]^{r_i} \tag{8}$$

When the interval for failure inspection is extremely small in such a way that a failure is detected in real-time, (8) becomes

$$L(p; t_1, \ldots, t_k) \propto \prod_{i=1}^{k} [f(t_i)]^{d_i} [1 - F(t_i)]^{r_i} \tag{9}$$

where $f(\cdot)$ is the pdf of t_i.

Any local minima in the objective function should be avoided during optimization. Before starting the optimization process, sweeping unknown variables in the calibration domain can be used to check if any local minima exist.

The optimization is an iterative process. Each iteration requires the execution of an Finite Element Analysis (FEA)

TABLE II
FAILURE MECHANISMS, SITES, AND MODELS FOR ELECTRONIC PACKAGING

Failure mechanisms	Failure sites	Failure lifetime models	References
Fatigue	Die attach, wire bond, solder joint, vias, pin-through-hole	$N_f = C\left(\Delta\varepsilon_p\right)^m$ N_f is the mean cycles to failure; $\Delta\varepsilon_p$ is the plastic strain change; c and m are the constants estimated by fitting data from experiments and finite element analysis.	Coffin-Manson [32]
Corrosion	Metallization	$t_f = A_C\left(RH\right)^{-n}\exp\left(\frac{E_{aC}}{kT}\right)$ t_f is the mean time to failure; A_C is a scale factor; n is a constant; RH is the relative humidity; E_{aC} is the activation energy for corrosion.	Peck [33]
Electromigration	Metallization	$t_f = A_{EM}\left(I - I_{crit}\right)^{-n}\exp\left(\frac{E_{aEM}}{kT}\right)$ t_f is the mean time to failure; A_{EM} and n are constants; I_{crit} is the critical current density; E_{aEM} is the activation energy for electromigration.	Filippi [34]
Conductive filament formation	Between metallization	$t_f = \frac{af\left(100L_{eff}\right)^n}{V^m\left(M - M_t\right)}, M > M_t$ t_f is the mean time to failure; a, f, n and m are the constants obtained from fitting experimental data; V is the applied voltage bias; M is the percentage moisture content; M_t is a percentage threshold moisture content; L_{eff} is the effective length between conductors.	Rudra [35]
Stress migration	Metal trace	$t_f = A_{SM}\left(\sigma\right)^{-n}\exp\left(\frac{E_{aSM}}{kT}\right)$ t_f is the mean time to failure; A_{SM} is a constant; σ is the mechanical stress; n is 2 to 3 for ductile metals; E_{aSM} is the activation energy for surface inversion	d'Heurle [36, 37]
Time dependent dielectric breakdown	Dielectric layer	$t_f = A_{TDDB}\exp\left(-\gamma E_{OX}\right)\exp\left(\frac{E_{aTDDB}}{kT}\right)$ t_f is the mean time to failure; A_{TDDB} is the metal-oxide semiconductor technology dependent constant; γ is the field-acceleration factor (cm/MV); E_{OX} is the externally applied electric field across the dielectric (MV/cm); E_{aTDDB} is the activation energy for time-dependent dielectric breakdown (TDDB)	Chowdhury [36, 38]

$(2N+1)$ or $(4N+1)$ times. Then, the EDR method can construct the statistical distribution of the lifetime. It is worth noting that a gradient-based optimization, if employed, demands an extra cost for computing gradients at every iteration. When the iteration converges, an optimal set of parameters of pdfs of unknown variables is determined. Otherwise, an initial guess of unknown variables is updated. The uncertainty propagation and likelihood calculation are subsequently repeated until the convergence criterion is met, as shown in Fig. 1.

IV. IMPLEMENTATION: BOARD-LEVEL RELIABILITY

When the solder joint fatigue failure or board level reliability (BLR) of surface mount components is evaluated through an accelerated thermal cycling (ATC) test, the CTF are known to vary significantly due to the inherent manufacturing variation by solder joint geometries as well as the nonuniform testing conditions. The proposed approach is implemented to predict the variation in the actual accelerated testing data. It is to be noted that the lead-based eutectic solder is used in the implementation because of the well-established damage model.

A. Accelerated Thermal Cycling Test

Three types of thick-film rectangular chip resistors were used. For 6332-type resistors, the solder pad with the size of 1 mm was patterned on printed circuit boards to control the amount of solder used in the assembly. They were mounted on the PCB using the lead-based Sn37Pb eutectic solder, as shown in Fig. 2. The specification of the test specimens is summarized in Table III. For an ATC test [23], the solder joint

TABLE III
SPECIFICATION OF TEST SPECIMENS

Resistor type	6332	1005	0603
Resistor dimension	6.3 mm × 3.2 mm	1.0 mm × 0.5 mm	0.6 mm × 0.3 mm
Pad size	1.0 mm	0.6 mm	0.4 mm
Solder	Lead-based Sn37Pb		
PCB coupon size	137 mm × 63 mm × 1.54 mm	76 mm × 77 mm × 0.4 mm	76 mm × 77 mm × 0.4 mm
Number of chip resistors	48	108	108

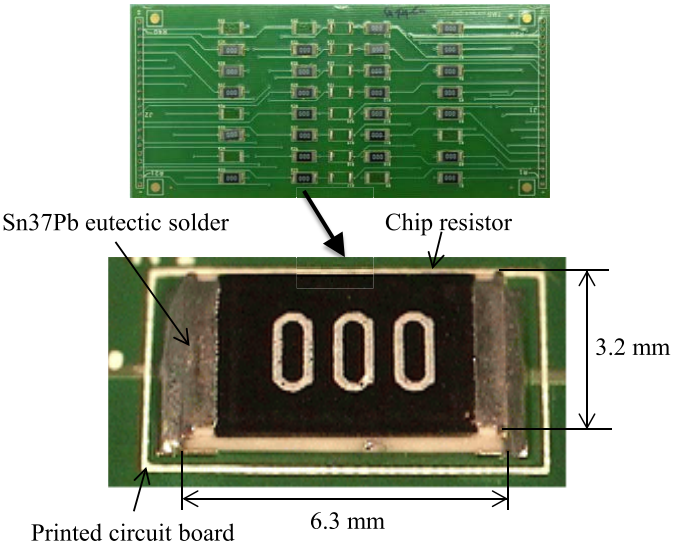

Fig. 2. 6332-type solder joint assembly used in ATC tests.

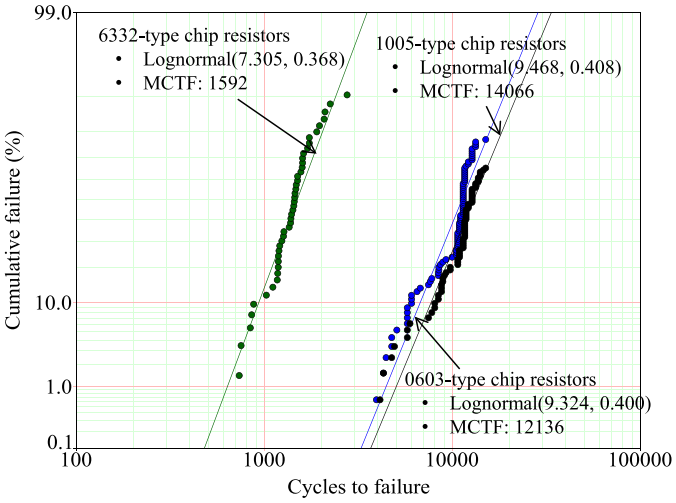

Fig. 3. Lognormal failure distribution plot of the ATC tests.

assemblies were subjected to temperature excursions from −50 °C to 125 °C. Each thermal cycle took 1 h, including a dwell time of 15 min.

Fig. 3 shows the distribution of lifetimes of the solder joint assemblies. The results were plotted using the lognormal distribution that provided the best fit to the CTF data. The 6332-, 1005-, and 0603-type solder joint assemblies have the mean cycles to failure (MCTF) of 1592, 14066, and 12136, respectively. The location and scale parameters of

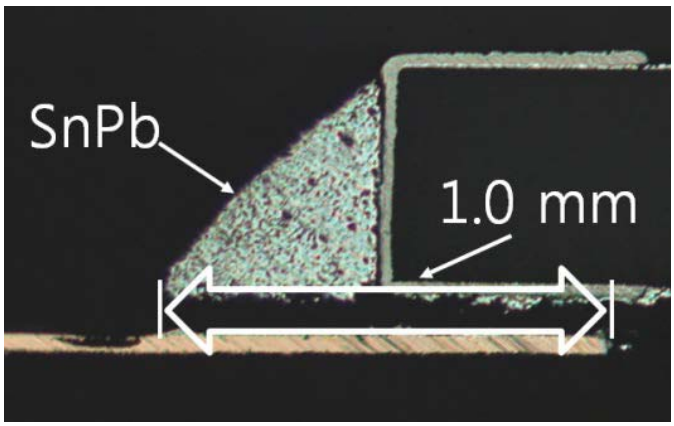

Fig. 4. Representative fatigue failure of solder joints in 6332-type solder joint assembly.

the three types of solder joint assemblies were (7.305, 0.368), (9.468, 0.408), and (9.324, 0.400). It was found that the scale parameter increased as the location parameter became large. The deviations in the CTFs were significant. For example, the cycles to 2% failure for the 6332-type solder joint assembly was estimated to be only around 700 cycles, while the cycles to 98% failure to be 3200 cycles.

The errors caused by ignoring censored data in the distribution analysis are shown in Tables IV–VI. As expected, the error increased as the percentage of censored data increased. Thus, it is inevitable to employ both the failure data and the censored data in a distribution analysis if a desired accuracy is required. For the same reason, the censored data should be incorporated in the likelihood analysis, which will be discussed in Section IV-C.

After the tests, a destructive failure analysis was conducted with failed solder joint assemblies. A representative example is shown in Fig. 4, which indicates that the dominant failure mechanism was is a typical fatigue failure in solder joints.

B. Solder Joint Fatigue Life and Damage Modeling

Darveaux's fatigue life model was employed to predict the fatigue lifetimes of the solder joint assemblies. The relationship between the strain energy density (ΔW_{ave}) and the CTF (N) has been known as

$$N_0 = K_1(\Delta W_{\text{ave}})^{K_2} \tag{10}$$

$$N_p = \frac{a}{K_3(\Delta W_{\text{ave}})^{K_4}} \tag{11}$$

TABLE IV
RESULTS OF 6332-TYPE SOLDER JOINT ASSEMBLY TEST DATA: 44 FAILURES AND 4 SURVIVALS (8.3% OF CENSORED DATA)

Data used in the distribution fitting		Failure and censored data (A)	Failure data only (B)	Error (={B-A}/A×100)
Mean cycles to failure		1592	1378	-13.4 %
Lognormal fitting	Location parameter	7.305	7.229	-1.0 %
	Scale parameter	0.368	0.278	-24.5 %

TABLE V
RESULTS OF 1005-TYPE SOLDER JOINT ASSEMBLY TEST DATA: 71 FAILURES AND 37 SURVIVALS (34.2% OF CENSORED DATA)

Data used in the distribution fitting		Failure and censored data (A)	Failure data only (B)	Error (={B-A}/A×100)
Mean cycles to failure		14066	10366	-26.3 %
Lognormal fitting	Location parameter	9.468	9.246	-2.3 %
	Scale parameter	0.408	0.293	-28.2 %

TABLE VI
RESULTS OF 0603-TYPE SOLDER JOINT ASSEMBLY TEST DATA: 84 FAILURES AND 24 SURVIVALS (22.2% OF CENSORED DATA)

Data used in the distribution fitting		Failure and censored data (A)	Failure data only (B)	Error (={B-A}/A×100)
Mean cycles to failure		12136	9641	-20.6 %
Lognormal fitting	Location parameter	9.324	9.174	-1.6 %
	Scale parameter	0.400	0.308	-23.0 %

where N_0 is the number of cycles to initiate cracks, N_p is the number of cycles to propagate cracks until failure, ΔW_{ave} is the net increase in the strain energy density per cycle, a is the crack size, and K_1, K_2, K_3, and K_4 are the empirical constants. The total lifetime for solder joint assemblies is the sum of N_0 and N_p. It has been known that N_0 for solder joint assemblies is much smaller than N_p [24]. Therefore, only (11) was used to estimate the solder joint lifetimes in this case study. In damage modeling, the strain energy densities in the solder joints were calculated using the viscoplastic model [25] in the commercial FEA package (VISCO107; ANSYS).

There is no established guideline on how to define the solder joint volume for the damage calculation (i.e., averaged inelastic strain energy density). The volume for averaging must be selected through investigating the failure mode of the actual test samples and the distribution of the inelastic strain energy. The geometry of solder joint assembly and the input variable to be calibrated (solder joint height) are illustrated in Fig. 5(a). The center layer of the solder joint elements below the chip resistor was used to average the strain energy density. The actual elements used to calculate the strain energy density and the inelastic strain energy density distribution in the solder joint are shown in Fig. 5(b) and (c), respectively. The thickness of a single layer of the mesh element used for averaging was 10 μm.

A preliminary analysis was conducted to establish a damage stabilization criterion; the damage was completely stabilized after four cycles. The average strain energy densities for the 6332-, 1005-, and 0603-type solder joint assemblies were 0.2569, 0.1600, and 0.1279 J/mm^2, respectively. The values of K_3 and K_4 were obtained by curve fitting of the strain energy densities and the MCTFs in Fig. 3 as 0.3884 and 4.7089.

C. Statistical Calibration Using EDR Method

The statistical calibration begins with the selection of unknown variables in the solder joint fatigue life model. The selection of an appropriate set of unknown variables is critical to the successful implementation of model calibration. Experimental evidence, sensitivity analysis, and engineering expertise on unrecognized model parameters can be used to decide unknown variables. In this paper, two unknown variables were identified from the literature review: 1) solder joint height variation and 2) temperature distribution in an environmental test chamber.

The first unknown variable, the solder joint height [Fig. 5(a)], is known to be very critical to BLR [26], [27]. Chai *et al.* [28] presented that both the solder joint height and the part tilt are the dominant factors that affect the solder interconnect reliability. According to [28], the solder joint height between the two sides of the same 6332-type resistor sample could vary as much as 12 μm when the nominal height was 30 μm.

The second unknown variable is the local temperature variation inside an environmental testing chamber. Verboven *et al.* [29] observed a large spatial distribution of the temperature during the end of the warm-up period in a forced convection oven; the measured average temperature was 181.3 °C and the standard deviation was 8.0 °C. At the steady state with the target temperature of 200 °C, the variability in the oven temperature reduced to 3.4 °C with the

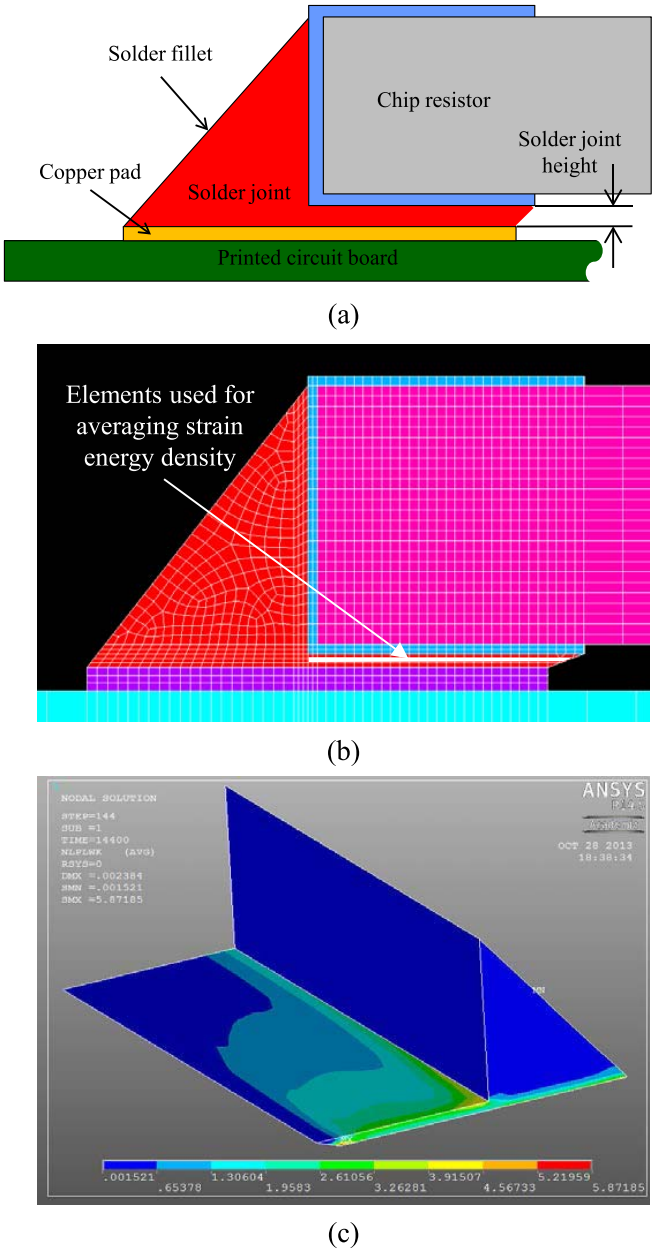

Fig. 5. Geometry of solder joint assembly. (a) Input variable to be calibrated (solder joint height). (b) Elements used to calculate strain energy density. (c) Inelastic strain energy density distribution in the solder joint.

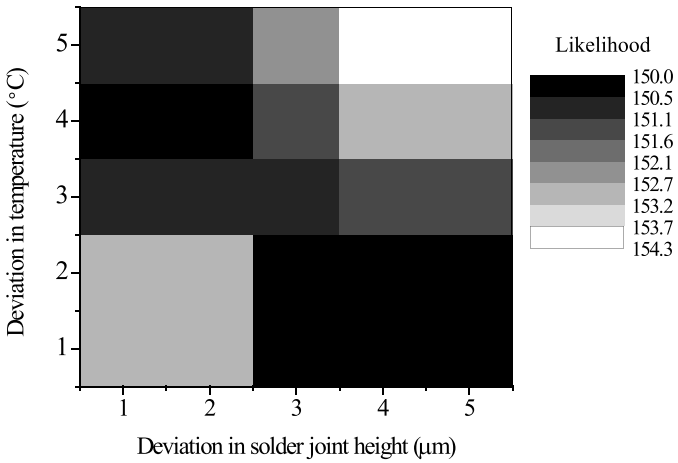

Fig. 6. Results obtained from a sweeping analysis to identify the local minima of the likelihood.

averaged measured temperature of 197.1 °C. A similar level of spatial temperature variation is expected in the ATC test.

The solder joint height was assumed to follow a lognormal distribution, since a negative value was not permitted, and the spatial distribution of the temperature in a convection oven was assumed to follow a normal distribution based on the analysis in [29]. As a result, three parameters of the pdfs were considered as unknowns for statistical calibration: 1) the location parameter of the solder joint height, 2) the scale parameter of the solder joint height; and 3) the standard deviation of the oven temperature. The initial guess of the solder joint height was 30 μm and its standard deviation was set to be 1 μm after reviewing the industrial standard [30]. The initial guess of the standard deviation of the oven temperature was 5 °C when the oven reached the maximum temperature of 125 °C.

A sweeping analysis was conducted first to identify any local minima in the likelihood function. As shown in Fig. 6, two potential local minima were observed for the standard deviations of solder joint height and oven temperature: 1) a combination of 1 μm and 4 °C and 2) a combination of 4 μm and 2 °C. The likelihood values at the local minima were 150.37 and 150.33, respectively, whose difference was negligible. The solder joint height deviation in the second combination (i.e., 22.9–38.6 μm with 95% confidence level) was unrealistic in the well-controlled soldering reflow process, i.e., this deviation exceeded the deviation in the worst case scenario [28]. Therefore, the first combination was considered as a proper starting point to be used in the statistical calibration.

A single run of the FEA based on the viscoplastic model took ~2 h. The EDR-based approximate integration technique required only $4N+1$ runs (i.e., nine runs when two unknown variables are considered, i.e., $N = 2$) for a single iteration. Multiple iterations are typically required, which result in additional computational time, e.g., 180 h (=10 × 9 runs × 2 h per run) for ten iterations. In this case study, the likelihood as well as the unknown variables completely converged after 14 iterations in the unconstrained optimization process using the "fmincon" function in MATLAB.

D. Results and Discussion

Fig. 7 compares the initial pdfs of the two unknown variables with the calibrated pdfs. In Fig. 7(a), the location parameter of the lognormal distribution for the solder joint height decreased from 3.401 to 3.376. Its scale parameter decreased from 0.033 to 0.009. The change in the scale parameter indicates that the deviation in the solder joint height is smaller than the initial guess. In Fig. 7(b), the standard deviation of the normal distribution for the oven temperature also decreased from 5.0 °C to 4.1 °C. This implies that a smaller amount of deviation in the solder joint height and the oven temperature was sufficient to accommodate the variability in the solder joint fatigue life. Fig. 8 compares

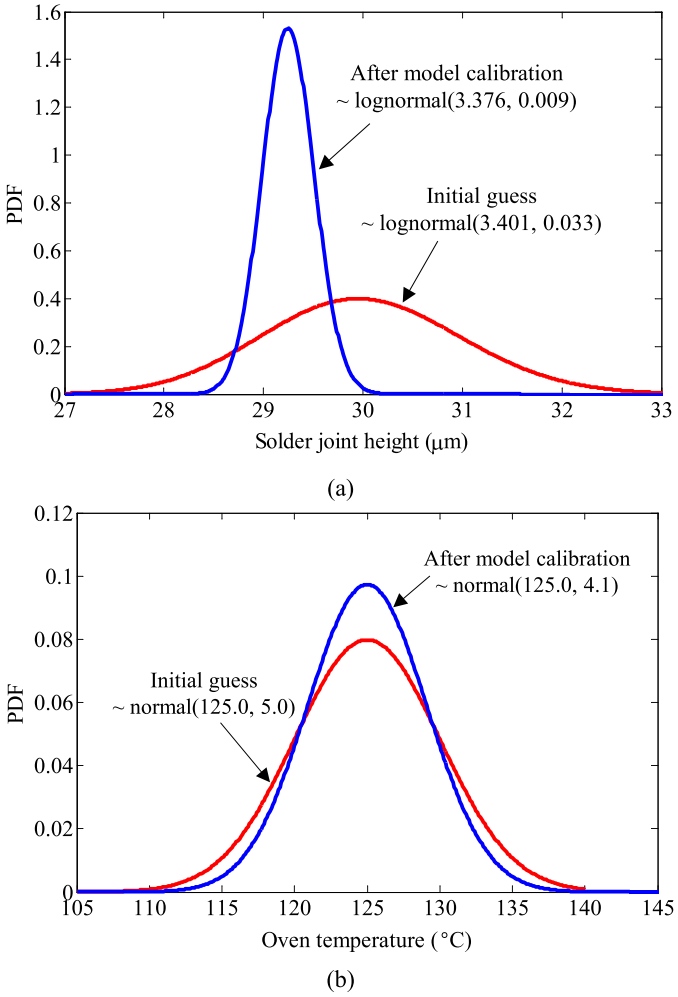

Fig. 7. Initial guesses and calibrated values for (a) solder joint height and (b) oven temperature.

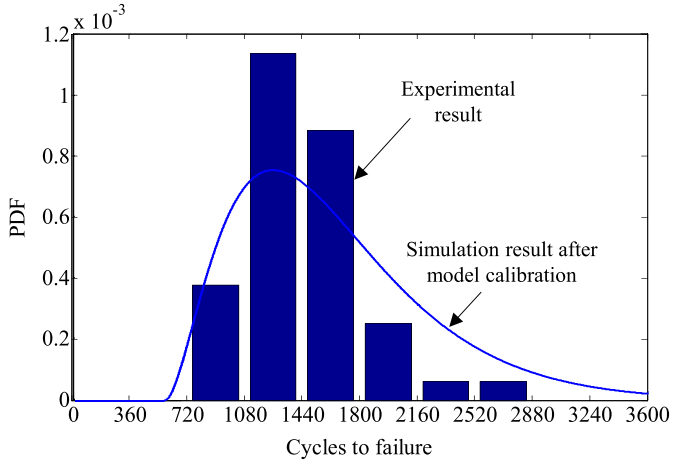

Fig. 8. PDF predicted from the calibrated model is compared with the experimental data.

the experimentally obtained lifetime histogram with the pdf predicted by the calibrated fatigue life model. The pdf shows good agreement with the histogram whose likelihood has been minimized with the value of 148.47.

A supplementary analysis was conducted to evaluate a case with only the solder joint height as an unknown variable

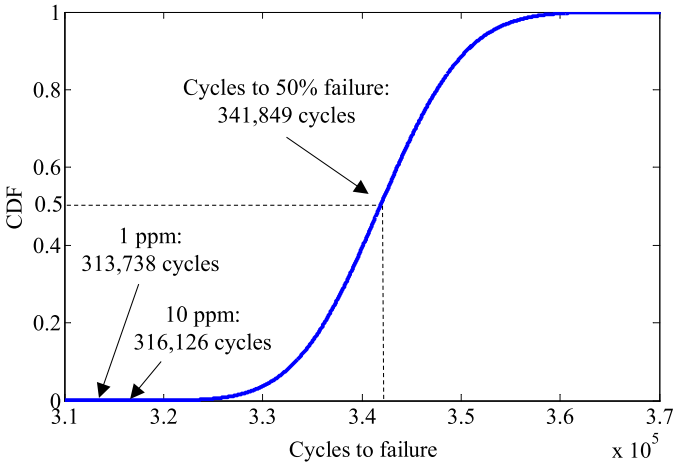

Fig. 9. Estimated BLR of portable electronics.

in the statistical calibration. After statistical calibration, the location and scale parameters of the lognormal distribution for the solder joint height were determined to be 3.370 and 0.116, respectively. With 95% confidence level, the solder joint height varies from 23.18 to 36.48 μm. The use of a single unknown variable leads to an unreasonably large deviation in the solder joint height, which is not physically feasible [28].

The reliability of the chip resistor used in portable electronics was predicted with the calibrated model. A field condition for the mobile device from IEC 60721-3-7 [31] includes the maximum and minimum temperatures of 70 °C and −40 °C. Fig. 9 shows the cdf of the solder joint fatigue life. The CTF for 1 and 10 ppm is 313738 and 316126 cycles, respectively.

V. Conclusion

A novel probabilistic lifetime prediction of electronic packages using the combined advanced uncertainty propagation analysis and model calibration was proposed. The proposed methodology consisted of: 1) an uncertainty propagation analysis using the EDR method; 2) a modified likelihood analysis to handle the failure data as well as censored data; and 3) an unconstrained optimization process to determine a calibrated parameter set of statistical distributions for unknown input variables.

The effectiveness of the proposed methodology was demonstrated by a case study of solder joint fatigue reliability. Uncertainties in the solder joint height in the chip resistor assemblies and the spatial distribution of the oven temperature were estimated while successfully overcoming the two challenges of typical electronic packaging applications: 1) the minimum computational cost without sacrificing the prediction accuracy and 2) the proper handling of the censored data. The calibrated model was further used to predict the reliability of solder joint assemblies under a field condition for the mobile device.

The results confirmed the computational effectiveness for an accurate physics-based lifetime model. It is anticipated that more probabilistic reliability problems of electronic packaging that have not been feasible due to excessive computational cost

will be implemented using the proposed methodology to be able: 1) to improve design and manufacturing processes and 2) to predict warranty and maintenance costs.

REFERENCES

[1] P. L. Hall and J. E. Strutt, "Probabilistic physics-of-failure models for component reliabilities using Monte Carlo simulation and Weibull analysis: A parametric study," *Rel. Eng. Syst. Safety*, vol. 80, no. 3, pp. 233–242, Jun. 2003.

[2] H. Oh, S. Choi, K. Kim, B. D. Youn, and M. Pecht, "An empirical model to describe performance degradation for warranty abuse detection in portable electronics," *Rel. Eng. Syst. Safety*, vol. 142, pp. 92–99, Oct. 2015.

[3] M. Chookah, M. Nuhi, and M. Modarres, "A probabilistic physics-of-failure model for prognostic health management of structures subject to pitting and corrosion-fatigue," *Rel. Eng. Syst. Safety*, vol. 96, no. 12, pp. 1601–1610, Dec. 2011.

[4] S.-P. Lee, J.-W. Jin, and K.-W. Kang, "Probabilistic analysis for mechanical properties of glass/epoxy composites using homogenization method and Monte Carlo simulation," *Renew. Energy*, vol. 65, pp. 219–226, May 2014.

[5] M.-L. Wu, "Assessing the impact of uncertainty in physics-of-failure analysis of microelectronics damage," *Mater. Sci. Eng. A, Struct. Mater. Properties Microstruct. Process.*, vol. 558, pp. 259–264, Dec. 2012.

[6] H. Oh, B. Han, P. McCluskey, C. Han, and B. D. Youn, "Physics-of-failure, condition monitoring, and prognostics of insulated gate bipolar transistor modules: A review," *IEEE Trans. Power Electron.*, vol. 30, no. 5, pp. 2413–2426, May 2015.

[7] J. W. Evans, J. Y. Evans, R. Ghaffarian, A. Mawer, K.-T. Lee, and C.-H. Shin, "Simulation of fatigue distributions for ball grid arrays by the Monte Carlo method," *Microelectron. Rel.*, vol. 40, no. 7, pp. 1147–1155, Jul. 2000.

[8] H. Janssen, "Monte-Carlo based uncertainty analysis: Sampling efficiency and sampling convergence," *Rel. Eng. Syst. Safety*, vol. 109, pp. 123–132, Jan. 2013.

[9] L. J. Ladani and J. Razmi, "Probabilistic design approach for cyclic fatigue life prediction of microelectronic interconnects," *IEEE Trans. Adv. Packag.*, vol. 33, no. 2, pp. 559–568, May 2010.

[10] D. G. Yang, J. S. Liang, Q. Y. Li, L. J. Ernst, and G. Q. Zhang, "Parametric study on flip chip package with lead-free solder joints by using the probabilistic designing approach," *Microelectron. Rel.*, vol. 44, no. 12, pp. 1947–1955, Dec. 2004.

[11] R. H. Myers and D. C. Montgomery, *Response Surface Methodology: Process and Product Optimization Using Designed Experiments*. New York, NY, USA: Wiley, 1995.

[12] S. Rahman and H. Xu, "A univariate dimension-reduction method for multi-dimensional integration in stochastic mechanics," *Probabilistic Eng. Mech.*, vol. 19, no. 4, pp. 393–408, Oct. 2004.

[13] B. D. Youn, Z. Xi, and P. Wang, "Eigenvector dimension reduction (EDR) method for sensitivity-free probability analysis," *Struct. Multidisciplinary Optim.*, vol. 37, no. 1, pp. 13–28, Feb. 2008.

[14] J. H. Gang, D. An, J. W. Joo, and J. H. Choi, "Uncertainty analysis of solder alloy material parameters estimation based on model calibration method," *Microelectron. Rel.*, vol. 52, no. 6, pp. 1128–1137, Jun. 2012.

[15] H. Oh, M. H. Azarian, C. Morillo, M. Pecht, and E. Rhem, "Failure mechanisms of ball bearings under lightly loaded, non-accelerated usage conditions," *Tribol. Int.*, vol. 81, pp. 291–299, Jan. 2015.

[16] *Guide for Verification and Validation in Computational Solid Mechanics*. New York, NY, USA: ASME, 2006, pp. 1–36.

[17] B. D. Youn, B. C. Jung, Z. Xi, S. B. Kim, and W. R. Lee, "A hierarchical framework for statistical model calibration in engineering product development," *Comput. Methods Appl. Mech. Eng.*, vol. 200, nos. 13–16, pp. 1421–1431, Mar. 2011.

[18] T. G. Trucano, L. P. Swiler, T. Igusa, W. L. Oberkampf, and M. Pilch, "Calibration, validation, and sensitivity analysis: What's what," *Rel. Eng. Syst. Safety*, vol. 91, nos. 10–11, pp. 1331–1357, Oct./Nov. 2006.

[19] F. Liu, M. J. Bayarri, J. O. Berger, R. Paulo, and J. Sacks, "A Bayesian analysis of the thermal challenge problem," *Comput. Methods Appl. Mech. Eng.*, vol. 197, nos. 29–32, pp. 2457–2466, May 2008.

[20] M. C. Kennedy and A. O'Hagan, "Bayesian calibration of computer models," *J. Roy. Statist. Soc. B (Statist. Methodol.)*, vol. 63, no. 3, pp. 425–450, 2001.

[21] Y. Xiong, W. Chen, K.-L. Tsui, and D. W. Apley, "A better understanding of model updating strategies in validating engineering models," *Comput. Methods Appl. Mech. Eng.*, vol. 198, nos. 15–16, pp. 1327–1337, Mar. 2009.

[22] W. Q. Meeker and L. A. Escobar, *Statistical Methods for Reliability Data*. New York, NY, USA: Wiley, 1998.

[23] C. Han and B. Han, "Board level reliability analysis of chip resistor assemblies under thermal cycling: A comparison study between SnPb and SnAgCu," *J. Mech. Sci. Technol.*, vol. 28, no. 3, pp. 879–886, Mar. 2014.

[24] H. Lu, C. Bailey, M. Dusek, C. Hunt, and J. Nottay, "Modelling the fatigue life of solder joints for surface mount resistors," in *Proc. Int. Symp. Electron. Mater. Packag.*, Hong Kong, Nov. 2000, pp. 136–142.

[25] H. R. Ghorbani and J. K. Spelt, "An analytical elasto-creep model of solder joints in leadless chip resistors: Part 2—Applications in fatigue reliability predictions for SnPb and lead-free solders," *IEEE Trans. Adv. Packag.*, vol. 30, no. 4, pp. 695–704, Nov. 2007.

[26] C. Y. Khor, M. Z. Abdullah, and W. C. Leong, "Fluid/structure interaction analysis of the effects of solder bump shapes and input/output counts on moulded packaging," *IEEE Trans. Compon., Packag., Manuf. Technol.*, vol. 2, no. 4, pp. 604–616, Apr. 2012.

[27] X. Liu and G.-Q. Lu, "Effects of solder joint shape and height on thermal fatigue lifetime," *IEEE Trans. Compon. Packag. Technol.*, vol. 26, no. 2, pp. 455–465, Jun. 2003.

[28] F. Chai, M. Osterman, and M. Pecht, "Reliability of gull-wing and leadless packages subjected to temperature cycling after rework," *IEEE Trans. Device Mater. Rel.*, vol. 12, no. 2, pp. 510–519, Jun. 2012.

[29] P. Verboven, N. Scheerlinck, J. De Baerdemaeker, and B. M. Nicolaï, "Computational fluid dynamics modelling and validation of the temperature distribution in a forced convection oven," *J. Food Eng.*, vol. 43, no. 2, pp. 61–73, Feb. 2000.

[30] *Acceptability of Electronic Assemblies*, IPC-A-610D, IPC Association Connecting Electronics Industries, Bannockburn, IL, USA, 2005.

[31] *Classification of Environmental Conditions—Part 3: Classification of Groups of Environmental Parameters and Their Severities. Section 7: Portable and Non-Stationary Use*, document IEC 60721-3-7, International Electrotechnical Commission, 2002.

[32] S. S. Manson, "Behaviour of materials under conditions of thermal stress," Nat. Advisory Committee Aeronautics, Washington, DC, USA, Tech. Rep. 1170, 1954.

[33] D. S. Peck, "Comprehensive model for humidity testing correlation," in *Proc. 24th Annu. IEEE Int. Rel. Phys. Symp.*, Anaheim, CA, USA, Apr. 1986, pp. 44–50.

[34] R. G. Filippi, G. A. Biery, and R. A. Wachnik, "The electromigration short-length effect in Ti-AlCu-Ti metallization with tungsten studs," *J. Appl. Phys.*, vol. 78, no. 6, pp. 3756–3768, Sep. 1995.

[35] B. Rudra, M. Pecht, and D. Jennings, "Assessing time-to-failure due to conductive filament formation in multi-layer organic laminates," *IEEE Trans. Compon., Packag., Manuf. Technol. B, Adv. Packag.*, vol. 17, no. 3, pp. 269–276, Aug. 1994.

[36] *Failure Mechanisms and Models for Semiconductor Devices*, document JEP122C, JEDEC Solid State Technology Association, Version C, Arlington County, VA, USA, 2006.

[37] F. M. d'Heurle and P. S. Ho, *Thin Films: Interdiffusion and Reactions*. New York, NY, USA: Wiley, 1978.

[38] N. A. Chowdhury, X. Wang, G. Bersuker, C. Young, N. Rahim, and D. Misra, "Temperature dependent time-to-breakdown (T_{BD}) of TiN/HfO_2 n-channel MOS devices in inversion," *Microelectron. Rel.*, vol. 49, no. 5, pp. 495–498, May 2009.

Hyunseok Oh received the B.S. degree from Korea University, Seoul, Korea, in 2004, the M.S. degree from the Korea Advanced Institute of Science and Technology, Daejeon, Korea, in 2006, and the Ph.D. degree from the University of Maryland, College Park, MD, USA, in 2012.

He was with the Hyundai MOBIS Technical Research Institute, Seoul, as a Research Engineer from 2006 to 2007. He was a Research Associate with the Center for Advanced Life Cycle Engineering, University of Maryland, from 2012 to 2014. He is currently a Research Professor with the Laboratory for System Health & Risk Management, Seoul National University, Seoul. His current research interests include prognostics and health management (PHM) and model verification and validation.

Dr. Oh received the A. James Clark Fellowship in 2007. He was a recipient of several awards, including the IEEE PHM Data Challenge Competition Winner in 2012, and the PHM Society Data Challenge Competition Winner in 2014 and 2015.

Hsiu-Ping Wei received the B.S. and M.S. degrees from the Department of Power Mechanical Engineering, National Tsing Hua University, Hsinchu, Taiwan, in 2005 and 2007, respectively.

He was a Senior Engineer with the Integrated Interconnect and Package Development Division, Taiwan Semiconductor Manufacturing Company, Hsinchu, where he was involved in zeroth level interconnection reliability under chip-packaging interaction. He is currently a Research Assistant with the Laboratory for Optomechanics and Micro/Nano Semiconductor/Photonics Systems, Center for Advanced Life Cycle Engineering, University of Maryland, College Park, MD, USA. His current research interests include probabilistic model verification and validation for microelectronics.

Bongtae Han is currently Key stone professor and APT chair of the Mechanical Engineering Department with the University of Maryland, College Park, MD, USA, where he directs the Laboratory for Optomechanics and Micro/Nano Semiconductor/Photonics Systems, Center for Advanced Life Cycle Engineering. He has co-authored a textbook entitled *High Sensitivity Moiré: Experimental Analysis for Mechanics and Materials* (Springer-Verlag, 1997), and edited two books. He has authored 12 book chapters and over 250 journal and conference papers in microelectronics, photonics, and experimental mechanics. He holds two U.S. patents and four invention disclosures.

Dr. Han was elected as a fellow of the Society for Experimental Mechanics (SEM) and the American Society of Mechanical Engineering (ASME) in 2006 and 2007, respectively. He received the IBM Excellence Award for Outstanding Technical Achievements in 1994. He was a recipient of the 2002 SEM Brewer Award for his contributions to the development of photomechanics tools used in semiconductor packaging. Most recently, he was named the 2016 ASME Mechanics Award Winner in the Electronic and Photonic Packaging Division for his contributions to the structural mechanics of electronic systems. His publication awards include the Year 2004 Best Paper Award of the IEEE TRANSACTIONS ON COMPONENTS AND PACKAGING TECHNOLOGIES, the Gold Award (best paper in the analysis and simulation session) of the First Samsung Technical Conference in 2004, and the Year 2015 Best Paper Award of the 16th International Conference on Electronic Packaging Technology. He served as an Associate Technical Editor of *Experimental Mechanics* from 1999 to 2001, and the *Journal of Electronic Packaging, Transactions of the ASME* from 2003 to 2012.

Byeng D. Youn received the B.S. degree from Inha University, Incheon, Korea, in 1996, the M.S. degree from the Korea Advanced Institute of Science and Technology, Daejeon, Korea, in 1998, and the Ph.D. degree from the University of Iowa, Iowa City, IA, USA, in 2001.

He was an Assistant Professor with the Department of Mechanical Engineering, University of Maryland, College Park, MD, USA. He is currently an Associate Professor of Mechanical and Aerospace Engineering with Seoul National University, Seoul, Korea. His research goal is to develop rational reliability and design methods based on mathematics, physics, and statistics for use in complex engineered systems, mainly focused on energy systems. His current research interests include reliability-based design, prognostics and health management (PHM), energy harvester design, and virtual product testing.

Dr. Youn's dedication and efforts in research have garnered substantive peer recognition resulting in notable awards, including the ASME IDETC Best Paper Awards in 2001 and 2008, the ISSMO/Springer Prize for a Young Scientist in 2005, the IEEE PHM Competition Winner in 2014, and the PHM Society Data Challenge Competition Winner in 2014 and 2015.